Control of Space Free-Flying Robot

Proceedings of the 29th Conference
on Decision and Control
Honolulu, Hawaii • December 1990

WA4 - 11:40

CONTROL of SPACE FREE-FLYING ROBOT

Kazuya Yoshida   and   Yoji Umetani

Department of Mechanical Engineering Science
Tokyo Institute of Technology
2-12-1, O-okayama, Meguro, Tokyo 152

ABSTRACT - This paper presents both theoretical and experimental study on the control of a free-flying robot manipulator for space application. The goal of the study is to develop a new control method for target capturing in space micro-gravity environment, considering the dynamical interaction between the manipulator operation and the base vehicle motion. In the theoretical study, Generalized Jacobian Matrix (GJM) concept for motion control and Guaranteed Workspace (GWS) for path planning, are investigated. In the experimental study, a laboratory model of robot satellite supported on air bearings is developed, which comprises a base satellite and a two-link manipulator arm. An on-line control scheme with vision feedback is developed for experimenting capture operations, on the basis of the GJM and GWS. The manipulator can properly chase and capture both a standing target and a moving target in spite of complex satellite/manipulator dynamical interaction.

1   Introduction

Space robotics is a new field. For a successful development of space projects, robotics and automation should be a key technology. Autonomous and dexterous space robots could reduce the workload of astronauts and increase operational efficiency in many missions. **Fig.1** shows a Japanese concept named COSMO-LAB's Free-Flying Robot [1]. One major characteristics of space robots, which clearly distinguishes them from on-earth operated ones, is the lack of a fixed base. Any motion of the manipulator arm will induce reaction forces and moments in the base, which disturb its position and attitude. If the arm were controlled for such task as target capturing without provision for this base disturbance, it would fail in the task.

To cope with this problem, the authors have been studying modeling and control of space manipulators since 1985. Generalized Jacobian Matrix (GJM) concept for motion control of the free-flying system, was developed. Resolved Motion Rate Control and Resolved Acceleration Control problems are treated in a similar way as for ground-fixed systems, by replacing the conventional Jacobian with the generalized matrix. On the other hand, for path planning, working area

of space manipulator is defined by analyzing free-flying behaviour of the space robots. These concepts are introduced in Chapter 2.

As for the experimental study, a laboratory model of robot satellite supported on air bearings is developed. An on-line control scheme with vision feedback is developed for experimenting capture operations, on the basis of the theoretical study. Control algorithm for the capture of both a standing and a moving target is developed in Chapter 3, and experimental results are presented in Chapter 4.

2   Dynamics and Kinematics

2.1   Modeling

Fig.2 shows a general model of space robot having a single manipulator arm, which is a free-flying serial $n + 1$ link system connected with n degrees of freedom active joints. The symbols are defined as follows:

$\mathbf{r}_i$: position vector of the mass center of link i

$\mathbf{p}_r$: position vector of a manipulator hand

$\mathbf{l}_i, \mathbf{a}_i, \mathbf{b}_i$: link vectors defined in **Fig.2**

m_i : mass of link i

w : total mass of the system ($= \sum_{i=0}^{n} m_i$)

$\mathbf{I}_i$: inertia tensor of link i with respect to the mass center of the link

$\boldsymbol{\omega}_i$: angular velocity vector of link i

Ω_0 : robot base attitude

Ω_n : robot hand attitude

$\boldsymbol{\phi}$: joint variables vector ($= (\phi_1, \phi_2, ..., \phi_n)^T$)

where $i = 0, 1, ..., n$. All vectors are defined with respect to the inertial coordinate system.
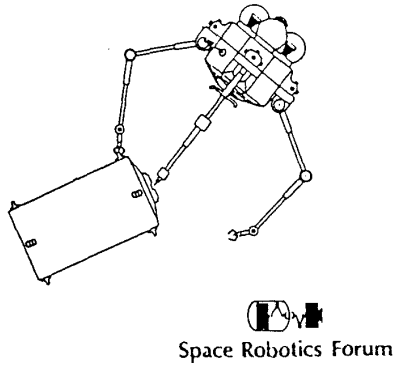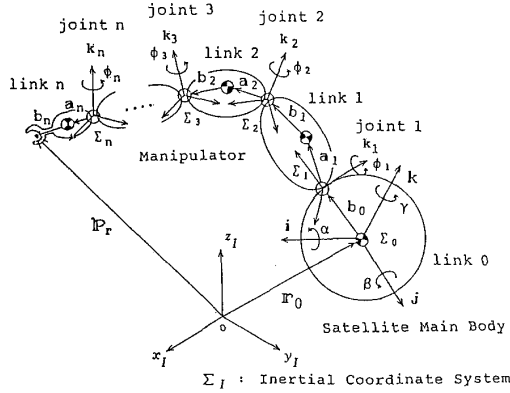
Fig.1 COSMO-LAB's Free-Flying Robot[1]

Fig.2 General model of space free-flying robot with an articulated manipulator

2.2 Equation of Motion

Let us define a generalized velocity of the system by translational and rotational velocities of the base satellite and joint velocities as $\dot{\mathbf{q}} = (\mathbf{v}_0^T, \boldsymbol{\omega}_0^T, \dot{\boldsymbol{\phi}}^T)^T$. Hence kinetic energy of the system T is

$$T = \frac{1}{2}[\mathbf{v}_0^T \, \boldsymbol{\omega}_0^T \, \dot{\boldsymbol{\phi}}^T]\mathbf{H} \begin{bmatrix} \mathbf{v}_0 \\ \boldsymbol{\omega}_0 \\ \dot{\boldsymbol{\phi}} \end{bmatrix} \quad (1)$$

where $\mathbf{H}(\boldsymbol{\phi})$ is the inertia matrix and $\mathbf{v}_0 \equiv \dot{\mathbf{r}}_0$.

Here, in the free-flying system with no external forces or moments, the variables $\mathbf{v}_0, \boldsymbol{\omega}_0, \dot{\boldsymbol{\phi}}$ are not independent. The manipulator motion induces the base satellite to rotate and translate, and momentum conservation law of the whole system gives "non-holonomic" constraint.

Translational and rotational momentum $\mathbf{P}, \mathbf{L}$ can be described as

$$\begin{bmatrix} \mathbf{P} \\ \mathbf{L} \end{bmatrix} = \mathbf{I}_s \begin{bmatrix} \mathbf{v}_0 \\ \boldsymbol{\omega}_0 \end{bmatrix} + \mathbf{I}_m \dot{\boldsymbol{\phi}} = 0 \quad (2)$$

with inertial parameters of the satellite part $\mathbf{I}_s$ and manipulator $\mathbf{I}_m$, assuming the total momentum is zero. This describes dynamic coupling between the manipulator operation and the base satellite motion. Equation of motion of the system is given by the Lagrange method with kinetic energy T and the constraint equation (2).

2.3 Generalized Jacobian Matrix (GJM)

Let us define a manipulator task space by position and orientation of the hand as $\mathbf{x} = (\mathbf{p}_r^T, \Omega_n^T)^T$. Kinematic equation of the manipulator hand at velocity level can be described with satellite and manipulator motion parts as,

$$\dot{\mathbf{x}} = \mathbf{J}_s \begin{bmatrix} \mathbf{v}_0 \\ \boldsymbol{\omega}_0 \end{bmatrix} + \mathbf{J}_m \dot{\boldsymbol{\phi}} \quad (3)$$

where $\mathbf{J}_s$ and $\mathbf{J}_m$ is Jacobian Matrix of the satellite and manipulator part respectively.

Now we can eliminate the variables $\mathbf{v}_0$ and $\boldsymbol{\omega}_0$ from (3) by substituting (2), then a relationship between the hand task space and the joint space is derived.

$$\dot{\mathbf{x}} = (\mathbf{J}_m - \mathbf{J}_s \mathbf{I}_s^{-1} \mathbf{I}_m)\dot{\boldsymbol{\phi}}$$

$$= \mathbf{J}^* \dot{\boldsymbol{\phi}} \quad (4)$$

The matrix $\mathbf{J}^*$, defined by the above equation, is Generalized Jacobian Matrix (GJM) [2] which represents manipulator kinematics and also implies free-flying dynamics of eq.(2). The main advantage of the GJM is that Resolved Motion Rate Control and Resolved Acceleration Control methods, which were developed for ground-fixed manipulators, are directly applied to space free-flying ones only by replacing the conventional Jacobian with the GJM [3]. In chapter 3, an on-line control scheme with vision feedback is developed for capture operation by using the GJM.

2.4 Two Joints System

Corresponding to the experimental model in the latter part, the following discussion will be hold on a two degrees-of-freedom plane model as shown in Fig.3. Here, the operational space $\mathbf{x}$ is represented only by the position of hand $\mathbf{p}_r$ and the kinematics is described as,

$$\mathbf{p}_r = K_0 \begin{bmatrix} c_0 \\ s_0 \end{bmatrix} + K_1 \begin{bmatrix} c_1 \\ s_1 \end{bmatrix} + K_2 \begin{bmatrix} c_2 \\ s_2 \end{bmatrix} \quad (5)$$

assuming the total mass center of the system lies on the origin of the inertial coordinate system, and symbols are as follows:

$$\begin{aligned}
K_0 &= m_0 b_0 / w \\
K_1 &= (m_0 l_1 + m_1 b_1)/w \\
K_2 &= \{(m_0 + m_1)l_2 + m_2 b_2\}/w \quad (6) \\
w &= m_0 + m_1 + m_2 \\
c_i &= \cos(\textstyle\sum_{j=0}^i \phi_i) \\
s_i &= \sin(\textstyle\sum_{j=0}^i \phi_i) \quad (i = 0, 1, 2; \quad \phi_0 = \Omega_0)
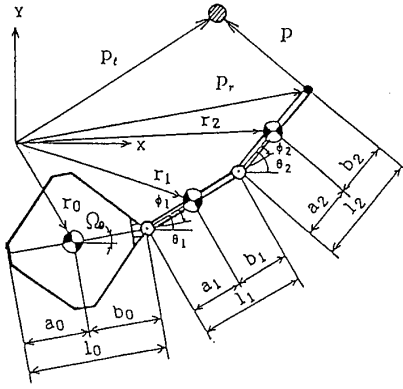\end{aligned}$$

98

Fig.3 Model for two joints free-flying robot
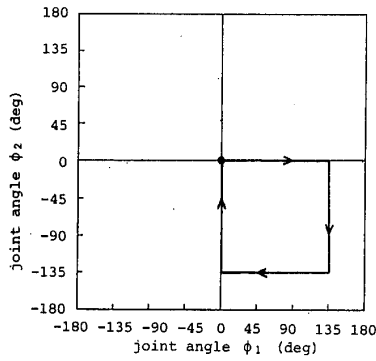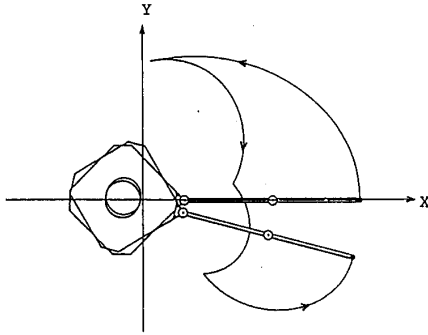

Fig.4(a) Cyclic operation in joint space

Fig.4(b) Non-holonomic behaviour by cyclic manipulator operation

By differentiating (5) with time, velocity-level kinematics is obtained as

$$\dot{\mathbf{p}}_r = \mathbf{J}_s \dot{\Omega}_0 + \mathbf{J}_m \begin{bmatrix} \dot{\phi}_1 \\ \dot{\phi}_2 \end{bmatrix}, \tag{7}$$

then the GJM is defined in the same way as (4).

$$\dot{\mathbf{p}}_r = \mathbf{J}^* \dot{\phi}$$

$$\mathbf{J}^* \equiv \mathbf{J}_m - \mathbf{J}_s \mathbf{I}_m / I_s \qquad \in R^{2 \times 2} \tag{8}$$

The definitions of $\mathbf{J}_s, \mathbf{J}_m, I_s, \mathbf{I}_m$ for this system are described in ref. [3].

2.5 Guaranteed Workspace (GWS)

In the free-flying robots, the locus of hand motion in the inertial task space depends on the history of joint operation. Let us illustrate this characteristic by a simple simulation. A set of cyclic operation in joint space is given as **Fig.4 (a)**. The simulated course of postural change and end-tip locus is shown in **Fig.4 (b)**. Notwithstanding the initial and final joint angles are the same, the position of hand in the inertial space becomes different. The one to one correspondence between the joint space and the inertial hand task space is not found: this is a typical feature of "non-holonomic" system.

The fact suggests that the reachability of the hand to a certain point depends on an approaching path, so that it cannot be discussed unless the path is specified, or other restrictions are provided.

To cope with this problem, the authors treat the working area in which no reachability limit is encountered. In the two joints system, reachable limit is given by $\phi_2 = 0$, where the manipulator arm is fully stretched into a singular posture. Substitute $\phi_2 = 0$ into (5), then

$$\mathbf{p}_r = K_0 \begin{bmatrix} \cos \phi_0 \\ \sin \phi_0 \end{bmatrix} + (K_1 + K_2) \begin{bmatrix} \cos \phi_1 \\ \sin \phi_1 \end{bmatrix} \tag{9}$$

is obtained, where the distance d from the origin (total mass center) to the hand is as

$$d = \sqrt{K_0^2 + 2K_0(K_1 + K_2) \cos \phi_1 + (K_1 + K_2)^2}. \tag{10}$$

In case of no restriction on ϕ_1, d is shortest at $\phi_1 = \pm \pi$, when eq.(9) gives a circle which center lies on $(0,0)$ with radius of $K_1 + K_2 - K_0$. In this circle, the hand is "guaranteed" to move from an arbitrary point to any point, without encountering the singularity of $\phi_2 = 0$. This area was previously defined in ref.[4] as "free workspace", however this paper proposes to name "Guaranteed Workspace (GWS)" to be explicit its meanings [5].

3 On-line Target Capture Control

3.1 Capture of Standing Target

An on-line Resolved Motion Rate Control (RMRC) scheme with a vision feedback is developed for the capture of a standing target by using the Generalized Jacobian Matrix (GJM). Suppose that the target lies still in GWS and following values are measured at each sampling interval δt

99

during the operation: Ω_0 - satellite attitude, ϕ_1, ϕ_2 - manipulator joint angles, $\mathbf{p}_r$ - position of manipulator hand, and $\mathbf{p}_t$ - position of the target.

Hand velocity command for the capture $\dot{\mathbf{p}}_{rd}$ is determined with a position error vector $\mathbf{p} = \mathbf{p}_t - \mathbf{p}_r$ by

$$\dot{\mathbf{p}}_{rd} = \frac{\mathbf{p}_t - \mathbf{p}_r}{\delta t}. \tag{11}$$

Operation command for the two joints $\dot{\phi}_d$ are obtained by the inverse of the GJM.

$$\dot{\phi}_d = [\mathbf{J}^*(\Omega_0, \phi_1, \phi_2)]^{-1}\dot{\mathbf{p}}_{rd} \tag{12}$$

If the calculated command is beyond a hardware limit $|\dot{\phi}_d| > \dot{\phi}_{max}$, then modify by

$$\dot{\phi}_d \leftarrow \frac{\dot{\phi}_{max}}{|\dot{\phi}_d|} \cdot \dot{\phi}_d. \tag{13}$$

3.2 Capture of Moving Target

In order to chase and capture a moving target, an optimum rendezvous trajectory is introduced. Let $\mathbf{p}_t$ be the position of target moving straightly at constant velocity and $\mathbf{p}_r$ the position of chaser, t_0 - the time starting the chase, t_f - the time of rendezvous. Define a cost function J as follows.

$$J = \frac{1}{2}(\mathbf{y}^T \mathbf{A} \mathbf{y})_{t_f} + \frac{1}{2}\int_{t_0}^{t_f} \ddot{\mathbf{p}}_r \mathrm{d}t \tag{14}$$

$$\mathbf{p} = \mathbf{p}_t - \mathbf{p}_r$$

$$\mathbf{y} = (\dot{\mathbf{p}}^T, \mathbf{p}^T)^T$$

$$\mathbf{A} = \mathrm{diag}(c_1, c_1, c_1, c_2, c_2, c_2)$$

$$(c_1, c_2 \to \infty)$$

A solution to minimize the cost (14) is theoretically known [6] as

$$\ddot{\mathbf{p}}_{rd}(t) = \frac{4}{t_f - t}\dot{\mathbf{y}} + \frac{6}{(t_f - t)^2}\mathbf{y}. \tag{15}$$

Integrating it with time, an optimum rendezvous trajectory is obtained, by which the chaser catches the target with no position or velocity error at the given time t_f with minimizing its acceleration.

However, this trajectory doesn't involve the constraint of chaser's motion. Here in fact, the chaser is a manipulator hand which has limited mobility and none at the singular configuration. For example, **Fig.5** shows target capture operation by using the ideal rendezvous trajectory (15). The manipulator encounters the singularity on the way of chase and fails in capture, because it works beyond the GWS. For manipulators installed on free-flying robots, the most important is to work within the Guaranteed Workspace.

It is difficult to solve the optimum rendezvous problem under the constraint of manipulator mobility, so the authors propose a practical method with on-line modification of the ideal solution.

1. Set the rendezvous time t_f, at which the target is in the GWS, on the assumption that the motion of target is predictable and the predicted target trajectory lies on GWS.

2. Solve an optimum hand acceleration by (15), then integrate it with time into velocity $\dot{\mathbf{p}}_{rd}$.

   (a) In case the hand is in GWS, $\dot{\mathbf{p}}_{rd}$ is a hand velocity command.

   (b) In case the hand is near or on the boundary of GWS, modify $\dot{\mathbf{p}}_{rd}$ to a tangent direction as shown in **Fig.6** by

   $$\dot{\mathbf{p}}_{rd} \leftarrow \dot{\mathbf{p}}_{rd} - (\frac{\dot{\mathbf{p}}_{rd} \cdot \mathbf{p}_r}{\|\mathbf{p}_r\|^2})\mathbf{p}_r \tag{16}$$

3. Resolve the hand velocity command into the joint command with the GJM by (12). If $|\dot{\phi}_d| > \dot{\phi}_{max}$, then the command must be modified by (13).

4. Repeat the control process 2. and 3. until the hand meets the target.

In the above proposed control scheme, the advantage as an optimum solution to minimize the cost (14) may be lost, however the mobility of hand is always guaranteed. The scheme is an RMRC at velocity level, and resolved acceleration scheme will also be developed in the same way as above.
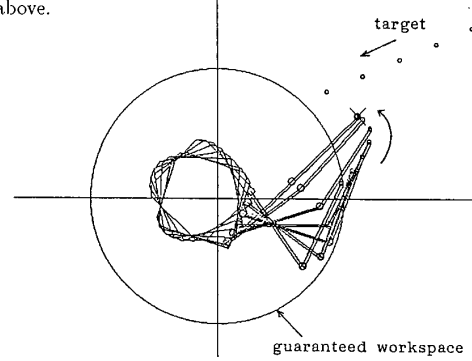

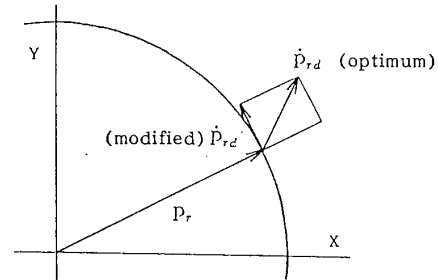**Fig.5** Target capture with no consideration of Guaranteed Workspace

Fig.6 Proposed modification of optimum rendezvous trajectory

100

4 Experiment

4.1 Design and Development of Laboratory Model

A laboratory model has developed for the experimental study. It is a serious problem for ground test experiments of space assemblies to simulate micro-gravity environment. In general, the following methods could be available.

1. Experiment in an airplane flying along a parabolic trajectory or a free-falling capsule. In this case, we can observe pure mechanical behavior under the law of nature, but it costs a lot and is inconvenient.

2. Experiment in a water pool with the support of neutral buoyancy. This is especially good for training of astronauts' activities.

3. Experiment on an air-cushion or air-bearings. In this case, however, the motion is restricted on a plane.

4. Calculate the motion which should be realize in micro-gravity environment by using a mathematical model, then force a mechanical model to move according to the calculation. This method is called as a 'hybrid' simulation combining mechanical models and mathematical ones.

Each method has advantages and disadvantages and, we should carefully select the method to satisfy the purpose of the experiment. Here, the present authors adopt the method No.3, because they would like to observe the behavior of mechanical link systems under the law of nature by the simplest apparatus.

A photograph of the developed model for this purpose is shown in **Fig.7**. A robot satellite model that has a 2 degrees-of-freedom manipulator, is supported by 3 pads with 1.5-2.0 kg/cm^2 of pressurized air. Each joint is actively rotated by a DC motor but no actuator for attitude control of the satellite base body. A target satellite with no manipulator is also floated by the air.

Hardware specifications and detail inertia parameters of the model are listed in **Table 1** and **2**.

The experimental model is evaluated to simulate acceleration environment as much as 10^{-3} of the earth gravitational acceleration [7].

The remote measurement and control system consists of wire-less communication port and PD servo-controller for on-board and CCD camera hanging from the ceiling, Video Tracker (VT) and personal computer (PC) for on-ground.

A block diagram for motion control is shown in **Fig.8**. The control loop is described as follows: Tip, joints and tail of the model and a target object are marked with light emitting diodes, and their motion is monitored by the CCD camera. Video signals of the LED marks are transformed into the position data p_t, p_r and the satellite attitude Ω_0
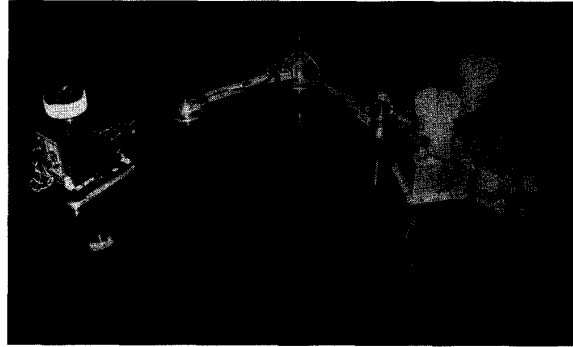

Fig.7 Photograph of the developed laboratory model

Table 1. Hardware specifications

Robot Satellite	
Satellite main body	
-dimension:	300x300mm
-weight:	6.3 kg
-on-board equipment:	
	gas-bomb type air supply
	rechargable batteries
	wireless communication system
	local servo-controller
Manipulator	
-dimension:	700mm (350mm for each link)
-weight:	1.4 kg
-actuator:	DC motor+planetary gear train
-sensors:	potentio-meters
	tacho-generators
Ground Equipment	
Planar base table	
-dimension:	1800x1800mm
-material:	planar glass
Measurement and control system	
-512x492 CCD camera (NEC)	
-Video Tracker (G-3100:OKK Inc.)	
-16bit personal computer (PC-9801-VX2:NEC)	

Table 2. Detail dimensions and inertia parameters of the model.

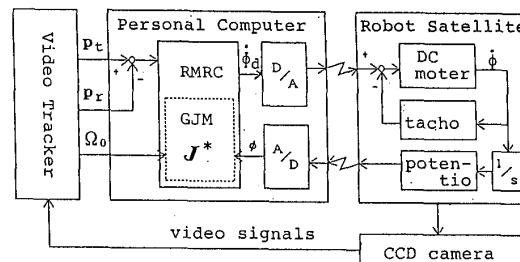| body	No.	0	1	2
a_i	[m]	0.190	0.162	0.124
b_i	[m]	0.190	0.188	0.226
m_i	[kg]	6.256	0.747	0.620
I_i	[kgm^2]	0.169	0.0424	0.0141

Fig.8 Control block diagram

101

by the VT and transmitted to the PC via a GPIB communication line. The control command $\dot{\phi}_d$ determined in the PC is transmitted to the robot via wire-less communication system. Manipulator joints are controlled with a local velocity feedback.

Conditions for the control is specified as:

maximum joint velocity $\dot{\phi}_{max}$: 15.0 deg/sec
data sampling interval δt : 0.1 sec

The calculation is executed by i80286+80287 processors using C language. Position sensing by the VT requires 1/30 seconds and near 0.05 seconds are spent for the calculation of the GJM and its inversion.

Note that the developed control scheme is based on the vision from the ground-fixed camera, however, it is equivalent to measure the position error between the hand and target by a satellite mounted (on-board) camera. It means that the scheme is applicable to fully on-boarded autonomous control system for space robots.

4.2 Capture of a Standing Target

Fig.9 shows a typical result of capture operation of a standing target. From the initial point to the target, the manipulator hand works straight and smoothly in spite of a complex satellite/manipulator dynamical interaction. This clearly shows the advantage of the GJM concept.

4.3 Capture of a Moving Target

Capture operations of a moving target are also successfully accomplished by the proposed on-line control method in section 3.2. **Fig.10** shows a typical result of the operation. The manipulator hand which was in the GWS at initial, is moving to left-up of the figure. However, near the boundary of GWS, the hand turns along to the circle, and finally it catches the target smoothly. In this experiment, the target moves irregularly by small external forces, nevertheless the hand successfully catches the target, because it is "on-line" controlled.

Experimental results shows the validity and availability of proposed control methods based on the GJM and GWS concepts.

5 Conclusion

This paper established the Generalized Jacobian Matrix and Guaranteed Workspace concepts for the control of space free-flying robots, through the theoretical and experimental investigation. The GJM guarantees proper manipulation and the GWS guarantees mobility of the hand, in spite of complex non-holonomic behaviour of the free-flying system.
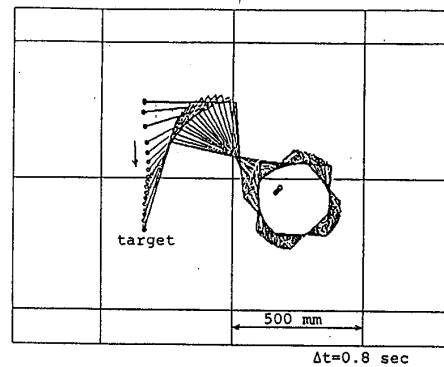

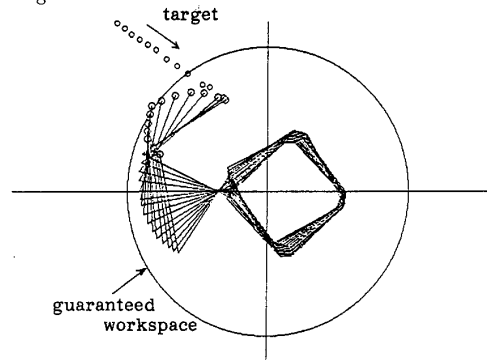**Fig.9** Experimenting capture operation of a standing target.

Fig.10 Experimenting capture operation of a moving target

6 Reference

[1] Y.Umetani: *Report of Research Forum on Space Robotics and Automation: Executive Summary*, Japan Space Utilization Promotion Center, 1990.

[2] Y.Umetani, K.Yoshida: "Continuous Path Control of Space Manipulator Mounted on OMV", *Acta Astronautica*, vol.15, No.12, pp.981-986, 1987.

[3] Y.Umetani, K.Yoshida: "Resolved Motion Rate Control of Space Manipulators with Generalized Jacobian Matrix", *IEEE Trans. on Robotics and Automation*, vol.5, No.3, pp.303-314, 1989.

[4] Z.Vafa, S.Dubowsky: "On the Dynamics of Manipulators in Space Using the Virtual Manipulator Approach", *Proc. of 1987 IEEE Int. Conf. on Robotics and Automation*, pp.579-585,1987.

[5] K.Yoshida: "Workspaces for Space Manipulators", submitted to *IEEE Trans. on Robotics and Automation*.

[6] T.Komatsu et al.: "Capture of Free-Flying Payloads with Flexible Space Manipulators", *Proc. NASA Conf. on Space Telerobotics*, 1990.

[7] Y.Umetani, K.Yoshida: "Theoretical and Experimental Study on In-orbit Capture Operation with Satellite Mounted Manipulators", *IFAC Automatic Control in Aerospace edited by Nishimura*, pp.121-126, 1989.